IUST Iran University of Science and Technology

Iranian Journal of Electrical and Electronic Engineering

Journal Homepage: ijeee.iust.ac.ir

2D DOA Estimation of Wideband and FH Signals Using Improved K-means Clustering and Implementation Considerations

Zahra Memarian* and Mahdi Majidi*(C.A.)

Abstract: This paper presents a two-dimensional (2D) direction of arrival (DOA) estimation method based on the popular correlative interferometer (CI) approach, incorporating practical considerations. Leveraging the flexibility of software-defined radio (SDR) platforms, the proposed array antenna model is designed according to the specifications of a dual-channel synchronous USRP B210 receiver and an appropriate RF switch. To enhance the speed and accuracy of 2D DOA estimation for narrowband, wideband (WB), and frequency hopping (FH) signals, this study introduces a method that integrates power spectrum density (PSD) and spectrogram analysis of the receiver's instantaneous bandwidth with an optimized filter bank, to precisely detect active frequencies and their intervals. Additionally, a fast, modified K-means clustering algorithm is developed to refine DOA estimation for FH and WB signals across multiple active subchannels. Simulation results demonstrate improved DOA estimation accuracy in multipath conditions, particularly at longer distances, with further enhancements achieved through the proposed clustering method.

Keywords: 2D DOA Estimation, Wideband, Frequency Hopping, Filter Bank, Modified K-means Clustering.

1 Introduction

DIRECTION finding (DF) systems, which use different methods for estimating the direction of arrival (DOA) of wireless radio frequency signals to a system, are widely used nowadays for applications such as monitoring and locating transmitters, improving wireless communications, etc. Among the famous DOA estimation methods, beamforming-based techniques such as Capon offer higher accuracy compared to classical methods, but their performance decreases in the presence of noise and calibration errors. More accurate subspace-based methods, such as MUSIC, also provide high accuracy but require a multi-channel receiver, increasing system cost and complexity. Additionally, sparsity-based or compressive sensing (CS) methods, while capable of estimating sources in scenarios with limited data, suffer from complex computations, resulting in lower speed and making them unsuitable for real-time applications [1-5]. In recent years, deep learning-based approaches, particularly convolutional neural networks (CNNs), have gained significant attention in DOA estimation. These methods leverage data-driven learning to extract complex spatial features, allowing for enhanced accuracy and robustness compared to traditional model-based techniques [6,7]. Meanwhile, the correlative interferometer (CI) method remains a widely adopted technique in direction-finding (DF) systems due to its high accuracy, computational efficiency, and cost-effectiveness. Unlike deep learning methods, which require extensive training datasets and computational resources, CI offers a straightforward implementation with minimal hardware complexity while maintaining reliable performance. As a result, it continues to be a preferred choice in practical applications where real-time processing and hardware constraints are critical considerations [1,4,8,9].

Iranian Journal of Electrical & Electronic Engineering, 2025.
Paper first received 01 Nov. 2024 and accepted 14 Jan. 2025.
* The authors are with the Department of Electrical and Computer Engineering, University of Kashan, Kashan, Iran.
E-mails: zahra.memarian@grad.kashanu.ac.ir, m.majidi@kashanu.ac.ir.
Corresponding Author: Mahdi Majidi.

Estimating the azimuth and elevation angles of the incoming wireless signal to an array, which is known as the 2D direction of arrival estimation, increases the efficiency and accuracy of DF systems. For example, to determine the position or better reception of the signals sent from flying objects such as drones or to estimate the DOA of signals emitted from different floors of a tall building, there is an essential need to determine the azimuth and elevation angles [1, 10, 11].

On the other hand, due to the expansion of the use of broadband and frequency hopping (FH) transmitters, it is of great importance to providing a suitable DF method to estimate the DOAs of these signals [12,13]. A common method for DOA estimation of wideband (WB) signals is to use a filter bank and apply a narrowband DOA estimation method to each subchannel of the desired filter bank. Then, using the information obtained from the frequency spectrum analysis, the results of the subchannels containing the desired WB or FH signal are averaged [1, 7, 14, 15]. Due to the dependence of the WB signals phase on the frequency and angle of arrival, the DOA results of each subchannel of the broadband signal are not exactly the same, and hence, the obtained results change around the original DOA of the signal. In addition, FH signals that change their frequency several times may be observed in multiple subchannels. Therefore, their DOA results are repeated frequently. However, the results obtained from these subchannels are not completely the same due to various reasons such as the presence of noise, or the limitations of the narrowband DOA method used in each subchannel. The high error of DOA results of some of these subchannels containing FH or WB signals can cause average deviation. Therefore, using the average method is not very accurate.

Another method is to use a histogram of the estimated DOAs of a WB signal. This graph, which can include any number of bins, performs better than the previous method. If these bins of angles are selected with a certain interval of the angular coverage in each category, the average results in the bin with the most members (i.e., the most recurring interval) are used to estimate the final DOA of the broadband signal. However, when the main angle of arrival is somewhere between the two bins of the graph, its accuracy is reduced [8, 16].

In recent years, the K-means clustering algorithm has been popular and widely in many applications used due to its simple implementation and low computational complexity [17-19]. In [20], the sub-band decomposition technique is used in WB signals, then DOA in each band is estimated using the ESPRIT method, and finally, the K-means method is used to obtain the DOA of wideband signal by clustering the results of each band. In [20], unlike the standard K-means algorithm in which the number of clusters must be specified and the initial clustering centers are randomly selected, an improved K-means clustering algorithm has been proposed to discover UAVs signals by analyzing the frequency spectrum, in which the number of clusters is selected by the density of data characteristics and the centers of the clusters are selected based on the maximum density. However, the cluster radius in this method is determined experimentally with repeated tests, and clustering is not related to DOA data.

Moreover, the use of software-defined radio (SDR) platforms based on field-programmable gate array (FPGA) cores with high-speed processing capability along with ease of implementation has attracted the attention of many designers and authors for use in real-time systems [22-26].

In this article, while using the two-dimensional (2D) geometry of the UCA array to estimate the elevation angle, through the expansion of the dictionary, the cost function of the improved CI method in [27] is modified and proposed in 2D form. Because of the widespread use of biconical antennas in broadband scenarios [28], the pattern of a designed biconical antenna is considered for the central element of the assumed array. Then, according to some other implementation considerations, including considering the characteristics of a suitable SDR along with a switch, the proposed DF system is proposed. After that, a K-means method is presented through the modification and generalization of the improved K-means method in [21]. The DOA results obtained in active subchannels containing FH and WB signals detected by power spectrum density (PSD) monitoring and instantaneous bandwidth spectrogram are clustered through the proposed K-means method.

This method reduces the error and determines the radius of the clusters without using repeated experiments along with only depending on the DOAs obtained in the real-time bandwidth of the receiver. The results of the simulations show the improvement of the elevation and azimuth angle estimation in terms of the SNR, the number of snapshots, and the DOA estimation accuracy of signals sent from far distances compared to the standard CI (SCI) method. Additionally, the better performance of the proposed modified K-means method for estimating the final DOA of FH and WB signals than the standard K-means, K-means++, and improved K-means methods in [21] is shown. The main contributions of this paper are as follows:

- Presentation of improved 2D cost function based on CI method.
- Presenting the DF system model considering technical specification of USRP B210 in designing the receiver parameters as an SDR.

- Presenting a model for identifying and estimating the bandwidth of NB, FH and WB signals and active in the IF bandwidth using PSD monitoring and real-time bandwidth spectrogram of the receiver with the aim of reducing calculations
- Peruse the optimal filter bank along with the presentation of the model for adjusting the number of switch rounds with the aim of collecting enough samples for DF processing, preventing frequency interference in active subchannels.
- Presenting a fast modified K-means method to estimate the final DOA of FH and WB signals.

Investigate the DOA results in the conditions of coherent, incoherent signals and multipath condition, checking the sensitivity to SNR and the effect of the distance from the proposed system on the estimation accuracy.

The second section of the article is about 2D DOA estimation, and the system model is explained in this section. The third section presents the DF system model and examines how to estimate the DOAs of the received signals with the assumption of a two-channel USRP B210 along with a single-pole nine-throw (SP9T) switch. In addition, calculations related to the received power, additive Gaussian noise power, identification of active subchannels with PSD monitoring and real-time bandwidth spectrogram of the receiver, and how to use the filter bank are dedicated to this section. The fourth section titled estimation of the final DOAs of FH and WB signals using the proposed modified K-means algorithm is related to the presentation of the proposed K-means method and the simulation results are presented in Section V. The conclusion is stated in Section VI.

2 2D DOA Estimation

Using the UCA array can not only provide DOA estimation with 360° unambiguous coverage but also can estimate the elevation angle using 2D geometry. Assuming a UCA with M directional elements and an omnidirectional element at its center as shown in Fig. 1, the system model will be described below.

2.1 System Model

Considering Fig. 1, the steering vector of the qth input source to the mth directional element of the array is defined as:

$$a_m(\theta_q, \varphi_q) = g_m(\theta_q, \varphi_q) e^{j\left(\frac{2\pi R}{\lambda}\right) sin(\theta_q) cos\left(\frac{(2\pi(m-1))}{M} - \varphi_q\right)}, \quad (1)$$

where R is the radius of the UCA, λ is the wavelength of the input signal, φ_q and θ_q are the azimuth and elevation angles of the qth input signal, respectively. According to [29] the normalized power pattern of the mth element in terms of elevation and azimuth angles is given by:

$$G_m(\theta_q, \varphi_q) = \frac{D(b)}{2^{2b}} (1 + sin\,\theta_q)^b \left(1 + cos\left(\varphi_q - \frac{2\pi(m-1)}{M}\right)\right)^b \quad (2)$$

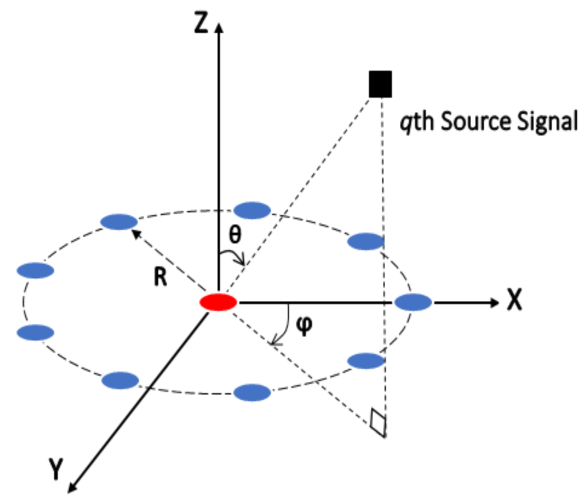

Fig. 1 Array model to estimate the azimuth and elevation angles of the input signals.

where $g_m(\theta_q, \varphi_q) = \sqrt{\left(G_m(\theta_q, \varphi_q)\right)}$, and b is directivity parameter. $D(b)$, which controls the directivity of the directional element, is defined in the following form.

$$D(b) = \frac{2^{2b+2}\pi}{\int_0^{2\pi}\int_0^{\pi}(1+sin\,\theta)^b(1+cos(\varphi))^b\, sin\,\theta\, d\theta\, d\varphi}. \quad (3)$$

For the central omnidirectional element shown in the array of Fig. 1, assuming a biconical broadband antenna, we use the radiation pattern of a designed biconical antenna. In Fig. 2, the three-dimensional (3D) radiation pattern of this antenna is displayed at 1 GHz frequency.

Additionally, Figure 3 shows the 3D radiation pattern of a directional element with a directivity parameter of 20 (b=20). Fig. 4 compares the radiation patterns of this element and a central biconical antenna, focusing on the elevation angle with the azimuth angle set to zero.

The output of the mth directional element located in the UCA perimeter in the nth snapshot is expressed as the following:

$$x_m(n) = \sum_{q=1}^{Q} s_q(n) a_m(\theta_q, \varphi_q) + w_m(n). \quad (4)$$

where $s_q(n)$ represents the qth narrowband signal source in the nth snapshot and $w_m(n)$ is the Gaussian complex white noise received in the mth element with zero mean and variance σ_w^2 in the nth snapshot. Therefore, the cost function of the 2D improved CI method can be rewritten

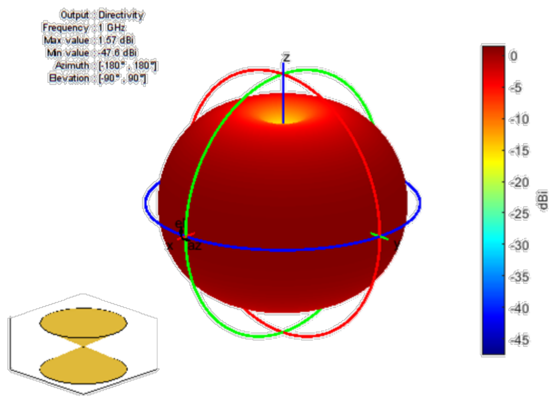

Fig. 2 The 3D radiation pattern of an omnidirectional biconical antenna.

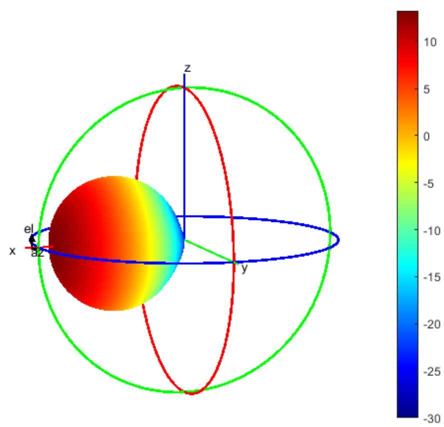

Fig. 3 The 3D radiation pattern of a directional element with the directivity equal to 20 (b=20).

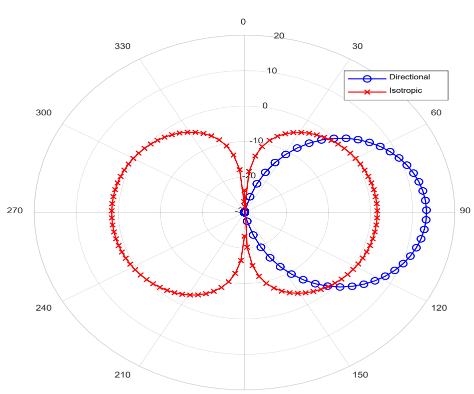

Fig. 4 Comparison of the vertical radiation pattern of the directional element with b=20 along with the omnidirectional biconical antenna. The azimuth angle is zero.

as below, considering the effect of elements gains.

$$J_{\mathrm{LS_{mdf}}}(\theta_i,\varphi_i) = -\sum_{m=1}^{M}\left[g_m(\theta_i,\varphi_i)\Big(\big((\Delta\phi_m(\theta_i,\varphi_i)+\pi) \bmod 2\pi\big)-\pi\Big)\right]^2, \qquad (5)$$

where mod is the modulo operator, and $\Delta\phi_m(\theta_i,\varphi_i)$ represents the mth element's phase difference with its corresponding phase in the lookup table. The lookup table is formed to cover all azimuth angles ($1° \le \varphi_i \le 360°$), and the proper elevation angle coverage is $60° \le \theta_i \le 90°$. Then the 2D DOAs will be obtained by calculating the peaks of the proposed improved cost function (5) in terms of the azimuth and elevation angles as shown in the following equation.

$$(\theta,\varphi) = \arg\max_{\theta_i,\varphi_i} J_{\mathrm{LS_{mdf}}}(\theta_i,\varphi_i). \qquad (6)$$

By combining the proposed 2D DOA method with the search region reduction (SRR) method in [27], it is possible to have a smoother 2D spectrum as well as increase the estimation speed.

3 DF of the Received Signal with USRP B210 Receiver and Using Filter Bank

In this section, the receiving and monitoring of the signals by the proposed array are investigated in four parts. The proposed DF system model with considering the specifications of a simultaneous two-channel USRP B210 receiver is introduced and analyzed in the first part. The second part is related to the computations of the received signal power and the calculations related to the additive noise power. In order to increase the speed and reduce the calculations, the proposed method of PSD monitoring and real-time bandwidth spectrogram of the receiver is presented in the third part, and the fourth part is dedicated to the analysis and use of the filter bank.

3.1 DF System Using Dual-Channel Synchronous USRP B210 Receiver Specifications with an Appropriate Switch

To present a cost-effective wideband DF system using the minimum number of simultaneous receiver channels, it is assumed here to use a USRP B210 dual-channel wideband receiver, with a real-time bandwidth of 30.72 MHz. The summary of the specifications of this receiver is listed in Table 1 [30].

Fig. 5 shows the proposed DF system model for the DOA estimation by the proposed array in the previous section together with using the USRP B210 dual-channel receiver. The first channel is connected to the biconical antenna while the second channel of this receiver can be switched between the directional elements using the SPxT switch. Here x should be equal to the number of directional elements used. It is worth noting that the samples are received synchronously from two channels.

Due to the necessity of collecting signals even with a short period of transmission time from all directions, the switch speed should be selected in such a way that the time duration of receiving from each directional element is as minimal as possible. Moreover, due to receiving at least one sample from each directional element, the maximum rate of the selective switch ($R_{\mathrm{sw}_{\max}}$) that changes from one position to another should be chosen less than or equal to the sampling rate of the receiver (R_{s}), which is mentioned below.

$$R_{\mathrm{sw}_{\max}} \leq R_{\mathrm{s}}. \tag{7}$$

As a result, according to the mentioned items, the sampling rate of the receiver and the switch time speed, the minimum number of samples received from each element (N_{spe}) during one round of switching will be obtained according to (8).

$$N_{\mathrm{spe}} = \frac{R_{\mathrm{s}}}{R_{\mathrm{sw}}}, \tag{8}$$

where N_{spe} is a positive integer value, so that the selective switch speed (R_{sw}) is a coefficient of the sampling rate and its maximum possible value, i.e., $R_{\mathrm{sw}_{\max}}$. Assuming 9 directional elements (M=9) and the USRP B210 receiver (R_{s}=30.72 MHz) as shown in Fig. 5, it is possible to use the SP9T switch model P9T-500M40G-60-R-55-292FF-OPT1222 with $R_{\mathrm{sw}_{\max}} = 10$ MHz [31]. As a result, N_{spe} will be equal to 4.

However, due to the use of a dual-channel receiver together with a switch, to receive a sufficient and reliable number of samples from each element for the DOA estimation of the received signals, the following two approaches are suggested:

3.1.1 Increasing the number of snapshots received from each directional element in one switch round:

By increasing the number of received samples or snapshots from each directional element in only one switch round and managing the received samples from the central element based on the received samples corresponding to each directional element, which are received simultaneously, the sampling rate of each element is maintained, and a sufficient number of samples will be obtained for DOA estimation. However,

Table 1. Specifications of USRP B210 synchronous dual-channel receiver [30].

Number	RF Performance		
1	Frequency range	70 to 6000	MHZ
2	Instantaneous bandwidth in 2x2	30.72	MHZ
3	Frequency sampling	61.44	MHZ
4	Receiver noise figure	< 8	dB

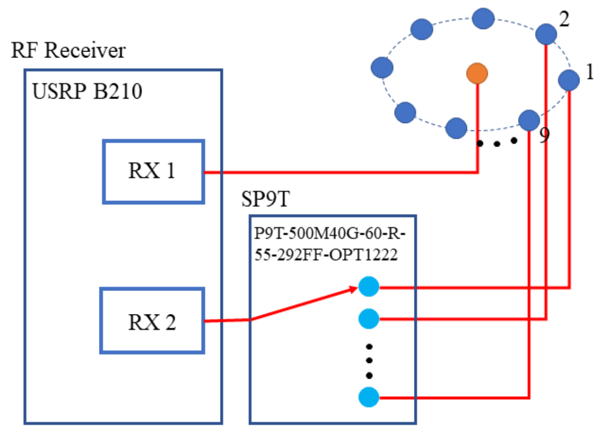

Fig. 5 The proposed DF system model

due to the long pause on each directional element, the system will not be able to find the direction signals with a transmission period shorter than the time of one switch round.

3.1.2 Setting the number of received snapshots from each directional element according to the number of switch rounds:

By creating a relationship between the number of snapshots received from each directional element in one switch round, and increasing the number of switch rounds to collect a sufficient number of snapshots for DF processing, this method could increase the speed of environment scanning while maintaining the sampling rate of the directional elements. In this way, the system will be able to collect signals with a shorter transmission period. Based on this method, the sufficient received number of samples or snapshots per element, is written as follows:

$$N_{\mathrm{spe}_{\mathrm{suff}}} = \eta_{\mathrm{Num}} \left(\frac{R_{\mathrm{s}}}{R_{\mathrm{sw}}}\right), \tag{9}$$

where η_{Num} is called the switch speed reduction coefficient, which is a suitable and arbitrary positive integer that should be chosen large enough.

3.2 Received Power and Additive Noise Power

In the calculations related to the additive noise power $\left(P_{\mathrm{Noise}_{\mathrm{dB}}}\right)$, the noise figure of the USRP B210 receiver is considered according to Table 1. Therefore, we have:

$$P_{\mathrm{AWGN}_{\mathrm{dB}}} = 10\log_{10}(kTB), \tag{10}$$

$$P_{\mathrm{Noise}_{\mathrm{dB}}} = P_{\mathrm{AWGN}_{\mathrm{dB}}} - P_{\mathrm{NF}_{\mathrm{dB}}}, \tag{11}$$

where $P_{\mathrm{NF}_{\mathrm{dB}}}$ is the noise figure of the receiver in dB, $P_{\mathrm{AWGN}_{\mathrm{dB}}}$ is the thermal noise power, k and T are Boltzmann's constant and the ambient temperature in Kelvin respectively, and B is the real-time bandwidth of the receiver. Additionally, the path loss ratio ($P_{\mathrm{L}_{\mathrm{dB}}}$) of each source at any distance from the proposed DF system for an urban area is defined from the following equation:

$$P_{\mathrm{L_{dB}}} = 10\alpha \log_{10}(d) + 20\log_{10}(f) + 32.4, \qquad (12)$$

where f is the signal frequency in MHz, d is the distance of the source from the array in km and α is the path loss exponent [32]. Therefore, the power received from a source in the receiver can be expressed as follows:

$$P_{\mathrm{r_{dB}}} = P_{\mathrm{tr}} - P_{\mathrm{L_{dB}}} - P_{\mathrm{SW}} - P_{\mathrm{VSWR}}, \qquad (13)$$

where P_{tr} is the transmitter power, P_{SW} and P_{VSWR} are insertion loss and VSWR loss related to the switch, respectively.

3.3 Calculation Reduction Using Monitoring of Instantaneous Bandwidth in PSD and Spectrogram

Because different transmitters are active in different frequency bands in the same environment, assuming the proposed DF system, the proposed DOA method should be applied to each frequency band. However, some frequency bands may not contain any strong and active signals, which increases the volume of calculation and waste time. Therefore, it is necessary to monitor the frequency spectrum of instantaneous bandwidth to detect the frequency band of active signals [1, 7].

According to Fig. 2, if the first receiver channel connected to the omnidirectional central element is used as the spectrum monitoring channel, the active frequencies are detected by detecting their energy in the instantaneous bandwidth of the USRP B210 receiver. Therefore, a threshold level, $T_{\mathrm{active_{dB}}}$, for detecting an active signal with sufficient energy in the smoothed PSD plot of the instantaneous bandwidth can be defined as the following equation:

$$T_{\mathrm{active_{dB}}} = \delta_{\mathrm{Th_{dB}}} + 10\log10\left(P_{\mathrm{Noise_{watt}}}/B\right), \qquad (14)$$

where $\delta_{\mathrm{Th_{dB}}}$ is a suitable integer.

By removing the constant frequency bands containing narrowband or WB signals from the active frequency bands, the frequency bands containing only FH signals can be determined. To achieve this goal, spectrogram monitoring of the instantaneous bandwidth of the receiver can be used to detect active constant frequency signals. The suggested steps are as follows:

- Median vector calculation (f_{median}): Median function calculation in each frequency bin in the short-time Fourier transform (STFT) matrix resulting from the instantaneous bandwidth spectrogram.
- Calculation of the Median smoothed vector ($f_{\mathrm{med-smooth}}$): Apply a Median filter with the appropriate degree to the median vector (f_{median}).

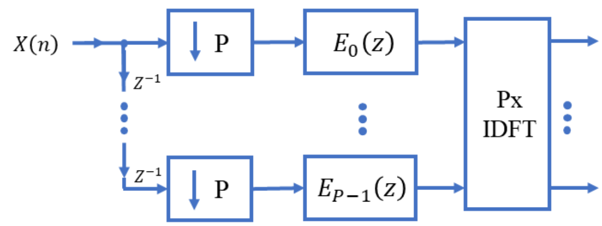

Fig. 6 P-length DFT or FFT bank with polyphase decomposition [15].

- $f_{\mathrm{med-smooth}}$ Analysis: Determination of active frequency bands containing constant frequency signals by defining a suitable threshold.

Additionally, WB signal frequency bands can be distinguished from active narrowband signal frequency bands by analyzing their energy levels across multiple consecutive frequency bands. If the energy remains consistent over adjacent bands, it indicates the presence of a WB signal rather than a constant frequency band.

Then, according to the detected active frequencies interval and the frequency range of each subchannel of the filter bank defined on the instantaneous bandwidth of the receiver (are determined only according to the number of desired subchannels before calculating the output of the subchannels), the active subchannels containing narrowband, WB and FH signals are determined.

3.4 Filter Bank

The filter bank divides the instantaneous bandwidth into smaller subchannels. However, in this article, according to the information obtained from PSD, based on the detection of active subchannels and applying this information to the filter bank, the filter bank output is calculated only in the active subchannels, then, by applying the proposed DF method to each subchannel, the DOAs in each subchannel are determined.

The primary implementation of the filter bank, which is done to enable the implementation of narrowband DF algorithms in each subchannel, is done by defining a symmetric low-pass filter and shifting the frequency of the input signal to the baseband. Then, the sampling rate is reduced. However, to reduce the computational complexity, including reducing the sampling rate before subchannels calculation, the optimal implementation of the filter bank can be used through filters with the polyphase structure. To implement a filter bank with P subchannels with separate outputs, polyphase structure and discrete Fourier transform (DFT) according to Fig. 6 are used, where $E_p(z)$ is the pth polyphase component of the primary low-pass filter. As a result, assuming the total number of snapshots is N, fewer snapshots (N/P) are used per subchannel, and calculations are performed faster. Finally, delays and decimation can be replaced with a commutator switch [15].

Considering the number of snapshots required for accurate or reliable DF processing in each subchannel (N_{re}), the total number of subchannels (P), preventing frequency interference, and satisfying the Nyquist rate in the active subchannels, the required number of switch cycles (N_{sc}) can be obtained as:

$$N_{\mathrm{sc}} = \frac{N_{\mathrm{re}}P}{N_{\mathrm{spe}_{\mathrm{suff}}}} \tag{15}$$

The filter bank divides the WB signal into several narrowband signals in different subchannels. Then the proposed DF method is applied to each subchannel. Here, the main challenge is to combine the DOA results of subchannels to estimate the final DOA of WB signals with higher accuracy.

4 Estimation of the final DOAs of FH and WB signals using the proposed modified K-means algorithm

In this section, a modified proposed algorithm based on the K-means clustering algorithm is proposed to estimate the DOA of WB and FH signals. Clustering is performed on the DOA estimation results of active subchannels containing FH and WB signals in the real-time bandwidth of the USRP B210 receiver, and unlike the standard K-means algorithm, the proposed method does not need to know the number of clusters or any other initial parameters.

Algorithm 1: Proposed modified K-means algorithm

Input: Estimated 2D DOA Matrix from active subchannels corresponds to FH/WB signals (D)
Step 1: Compute Euclidean distance matrix (d_{ij})
  Extract number of sources
  Compute d_{ij} for all 2D points
Step 2: Compute the minimum distance vector ($d_{\min}$)
  $d_{\min}(i) = \min(d_{ij}),\ \forall j \neq i$
Step 3: Find the max and min of $d_{\min}$
  $d_1 = \min(d_{\min})$, $d_2 = \max(d_{\min})$
Step 4: Calculation of R_{Clu}
  Normalize $d_{\min}$ by d_2
  w = mean (normalized $d_{\min}$)
  $R_{\mathrm{Clu}} = (1-w)\times d_1 + w\times d_2$
Step 5: Compute the density of each data object (h)
  $h(i) = length\ (\{j \mid d_{ij} \leq R_{\mathrm{Clu}},\ \forall j \neq i\})$
Step 6: Calculate center of the first cluster
  $center_1 = argmax(h)$
Step 7: Iterative cluster formation
  While D ≠ ∅:
    $C_k = \{x_i \in D \mid$ Euclidean distance $(x_i, \mathrm{center}_k) \leq R_{\mathrm{Clu}}\}$
    $D = D - C_k$
Step 8: Reassign data points to the nearest cluster centers
Step 9: Compute final DOAs of FH/WB signals
  Separation of single/double-membered clusters
  $(\theta, \varphi)_{\mathrm{FH/WB}}$ = mean (remaining clusters points)
Output: $(\theta, \varphi)_{\mathrm{FH/WB}}$

4.1 An Overview of K-means Algorithm

The K-means clustering algorithm is a subset of centroid-based hard/crisp partitional clustering algorithms in which the data is distributed based on their attributes into a specified number of clusters (K) where each data object becomes a member of only one cluster. K-means clustering as a centroid-based technique uses the mean function to represent the center of a cluster. In this method, the quality of the partition is evaluated by measuring the similarity of the data objects in one cluster (intra-cluster similarity) compared to the data of another cluster (inter-cluster similarity) [18].

At the start of the algorithm, after choosing the number of clusters (K), K data objects are randomly selected from the set of available data objects as initial representatives for the center of K clusters. Then the Euclidean distance between the remaining data objects and each initial center point is measured. Based on the obtained values each data object is assigned to the cluster with the shortest distance. In each iteration, after allocating all data objects, the mean of each cluster is recalculated and updated. This procedure is repeated several times until stability is achieved. The data clustering in the standard K-means algorithm or Lloyd's algorithm is described as follows:

$$S_i^{(t)} = \left\{y_h : \left\|y_h - m_i^{(t)}\right\|^2 \leq \left\|y_h - m_j^{(t)}\right\|^2 \forall j, j \neq i\right\}, \tag{16}$$

where $S_i^{(t)}$ is the ith cluster set at time t, y_h is the hth object, and $m_i^{(t)}$ is the given initial object or the mean of the ith cluster at time t. Then, in the update phase, the mean of the clusters at time $\hat{t}$ is calculated through the following equation:

$$m_i^{(\hat{t})} = \frac{1}{\left|S_i^{(t)}\right|} \sum_{y_j \in S_i^{(t)}} y_j\ , \tag{17}$$

where $\left|S_i^{(t)}\right|$ represents the number of members of the ith cluster at time t [33, 34].

The major problems identified with the K-means clustering algorithm include the necessity of defining the number of clusters and their centers at the beginning of the algorithm. It has been reported that the K-means algorithm is very sensitive to the initial selection of the centroid, so convergence cannot be guaranteed if it is chosen incorrectly. The K-means algorithm is also sensitive to outlier data objects that are forced into the clusters and distort the cluster means. In addition, it requires high memory space, and the number of iterations to obtain a stable distribution is unknown [17, 18].

4.2 Clustering results using the proposed modified K-means algorithm

Unlike the standard K-means algorithm, the cluster centers and their number are extracted by the proposed algorithm itself based on the characteristics of data density and maximum data density. In addition, the proposed K-means algorithm is executed only once and does not need to enter any manual parameters such as the parameter related to determining the radius (parameter w in [21]). Additionally, at the end of the method, the clustering is checked and updated in order to increase the accuracy of the data clustering in terms of the minimum distance of the data from the determined cluster centers. The steps of the method are as follows:

Step 1: Calculate all Euclidean distances between the estimated 2D DOAs in active subchannels containing FH and WB signals.

Step 2: Determine the minimum distance of each data object to all other data objects and construct the minimum distance vector ($d_{\min}$).

Step 3: Calculate the maximum (d_2) and minimum (d_1) values of the minimum distance vector calculated in the previous step.

Step 4 (proposed): First, the minimum distance vector should be normalized by dividing it by its maximum value (d2). Then, the parameter w is defined as the average of the normalized vector. This parameter acts as a weighting factor, balancing the influence of the minimum and maximum distances within the minimum distance vector. Finally, the cluster radius is computed using the following equation, where w determines the relative contribution of d_1 and d_2:

$$R_{\mathrm{Clu}} = (1 - w) \times d_1 + w \times d_2 \tag{18}$$

Step 5: Compute the density of each data object h as the number of other objects within a distance of R_{Clu} from h.

Step 6: The data object with the highest density is selected as the center of the first cluster.

Step 7: Subsequent clusters are formed by removing the members of the previous cluster from the dataset and repeating the process until all data objects are clustered.

Step 8 (proposed): After clustering is completed, recompute the distances of all data objects to the centers of the obtained clusters. Each data object is reassigned to the cluster whose center is closest to it, ensuring an updated and refined clustering process.

Step 9 (proposed): Single or double-membered outlier clusters are considered narrowband sources and excluded from the final DOA estimation of WB and FH signals. Then, the mean is obtained for each cluster.

All the mentioned steps are summarized in pseudocode in Algorithm 1.

By matching the information obtained from the instantaneous bandwidth of the receiver, such as the number of subchannels containing broadband and FH signals, with the final DOAs calculated by the proposed K-means method, the DOA of each WB or FH signal observed in the receiver's instantaneous bandwidth will be determined.

5 Simulation Results

In this section, the simulation results of the proposed methods in the previous sections are presented. The simulations have been done by MATLAB software and in all experiments, the system array is similar to Fig. 1 with 9 directional elements (M=9) and an omnidirectional biconical antenna (Fig. 2) in the center of the UCA. The directivity parameter of directional elements is equal to b=20. Therefore, the estimation of the elevation angle is valid between 60° and 90°. Moreover, the receiver of the DF system is similar to Fig. 5, assuming the specifications of a dual-channel synchronous USRP B210 receiver and the aforementioned SP9T switch. The radius of UCA is equal to half the wavelength of the central frequency of the receiver bandwidth. The total number of subchannels is equal to P=80, $\eta_{\mathrm{Num}} = 600$, $\alpha = 3$ and $\delta_{\mathrm{Th_{dB}}}$ is equal to 10dB. The degree of Median filter stated in section 3.3, is considered to be 7. Since the SCI method uses omnidirectional elements, instead of the directional elements located on the UCA perimeter, the radiation pattern of 9 dipole elements is considered for it in simulations.

5.1 2D DOA Simulation Results Using the Proposed Cost Function

In this section, the performance of the cost function of the proposed DF method in (5) for 2D DOA estimation of several uncorrelated sources and a single source in multipath conditions is evaluated by the assumed DF system model based on Fig. 5.

5.1.1 Incoherent sources

This experiment has been performed assuming two incoherent narrowband sources at 2.41 GHz frequency and the resolution of the proposed 2D DOA method (2D PCI, which stands for 2D proposed correlative interferometer), along with the SRR method in [27] has been compared with the SCI method. The azimuth angles of these two assumed signals are 30° and 170°, respectively, and their elevation angles are equal to 70° and 80°. The sources are located at a distance of 700 meters from the receiver and their transmission power is equal to 1mW. The signals have QPSK modulation with root-raised cosine (RRC) pulse shape and their symbol

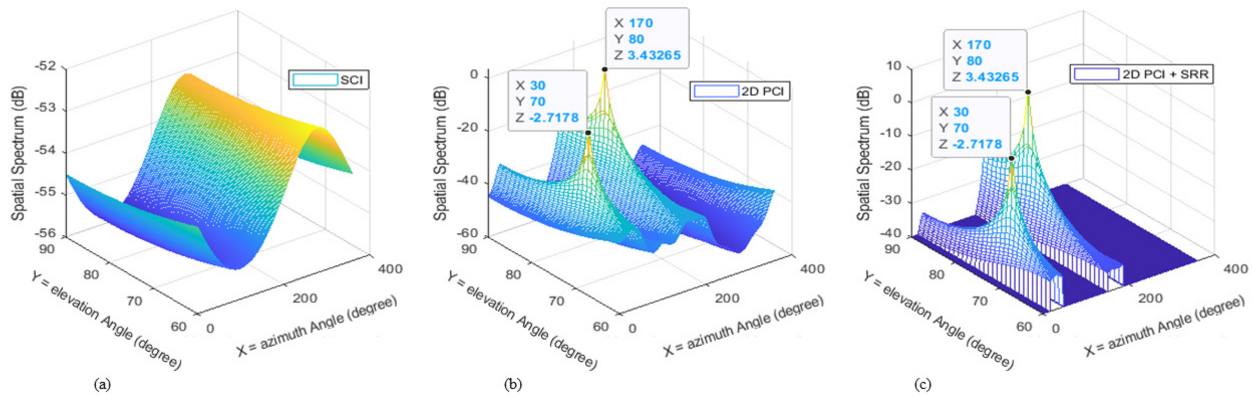

Fig. 7 The comparison of the 2D spatial spectrum of three methods when there are two incoherent input signals. (a) SCI method using lookup table expansion, (b) 2D PCI method, (c) 2D PCI + SRR method.

rate is 153.6 ksymb/s. The number of snapshots is equal to N_{re}=501.

Fig. 7 shows the 2D spatial spectrum of the SCI method using lookup table expansion (a), the proposed method (2D PCI) (b), and the proposed method together with SRR (2D PCI + SRR) (c) in estimating two incoherent input signals. Their azimuth angles are equal to 30˚ and 170˚, and their elevation angles are equal to 70˚ and 80˚, respectively.

According to Fig.7, it can be seen that the SCI method has completely failed in estimating and distinguishing the DOA of two sources, while 2D PCI and 2D PCI + SRR methods are succeeded.

5.1.2 Coherent sources

Sensitivity to SNR

Assuming a multipath scenario, a narrowband signal source and its reflection with half the power of the original signal are considered. Their DOA along the azimuth angle is 45˚ and 180˚, and along the elevation angle is equal to 80˚ and 90˚, respectively. Fig. 8 shows the performance of the proposed methods compared to SCI with LS criterion and SCI with Cos criterion in the form of root mean square error (RMSE) representation against different SNRs with 1000 independent Monte Carlo simulations. Other parameters are set as before.

As can be seen in Fig. 8, the negative slope of the plots of the proposed methods in the estimation of azimuth and elevation angles indicates an increase in estimation accuracy with the increase of SNR. In contrast, the slope of SCI method plots with both LS and Cos criteria are close to zero at high SNRs, and hence, there is the almost constant error due to the multipath phenomenon, and this error is more obvious in the estimation of the elevation angle.

Source distance effect on DOA estimation accuracy

Assuming the previous scenario, in this experiment, the performance of the proposed method along with the proposed DF system is compared with SCI methods in the case of different source distances from the array. Experiments at each source distance are performed with 1000 independent Monte Carlo trials. It can be seen in Fig. 9 that the proposed 2D PCI and 2D PCI with SRR methods using the array including directional elements perform better in estimating the source with further distances in the multipath scenarios.

In other words, the proposed DF system can cover a wider area. For example, at a distance of about 11 km from the array in Fig. 9(a), the proposed method compared to the SCI method with Cos and LS criteria is improved by 75.5% and 95.9%, respectively. Moreover, according to Fig. 9(b), it is clear that the estimation of the elevation angle in the multipath environment using SCI methods does not have the necessary accuracy and sensitivity and the results are not reliable.

5.2 2D DOA Estimation of Multiple Signals in Real-Time Bandwidth of USRP B210 Receiver Using Proposed DF System and Methods

In this experiment, assuming multiple narrowband, WB, and FH signals are received in the real-time bandwidth of the receiver, the proposed 2D PCI method is used to estimate the DOA of each of these signals in active subchannels of the filter bank.

The simulation results show the improvement of the DOA estimation results using the 2D PCI method compared to the SCI method in active subchannels containing more than one active signal. The assumptions of this scenario are as follows:

- Two coherent narrowband signals (original source and its reflection) with 20˚ and 185˚ azimuth angles: Their elevation angles are equal to 70˚ and 80˚, respectively. The carrier

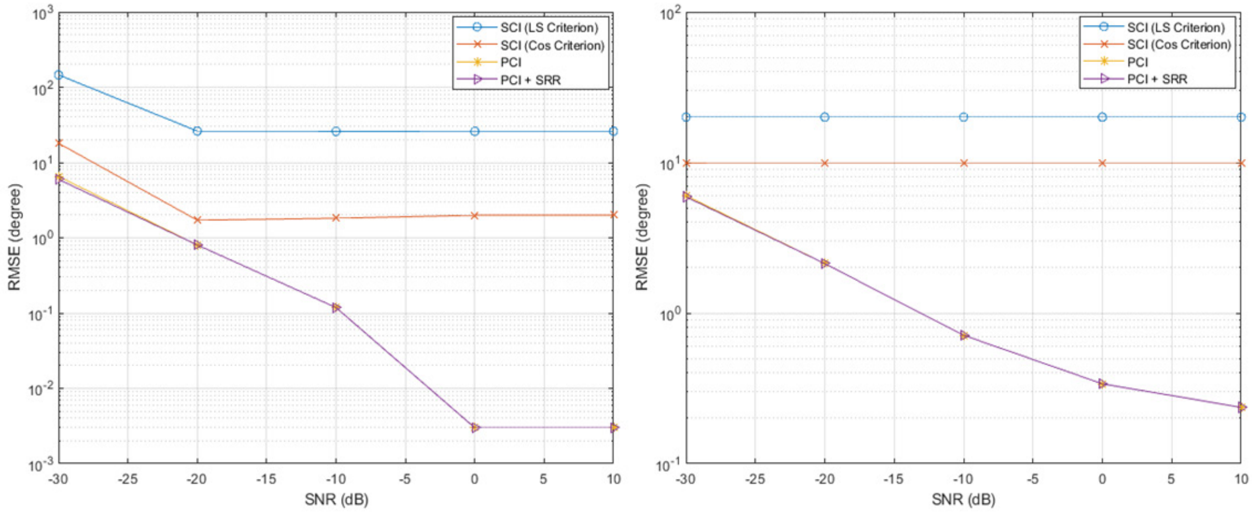

(a) (b)

Fig. 8 RMSE versus SNR using SCI with LS and Cos criteria, 2D PCI and 2D PCI + SRR methods in a multipath scenario. (a) Azimuth angle, (b) Elevation angle.

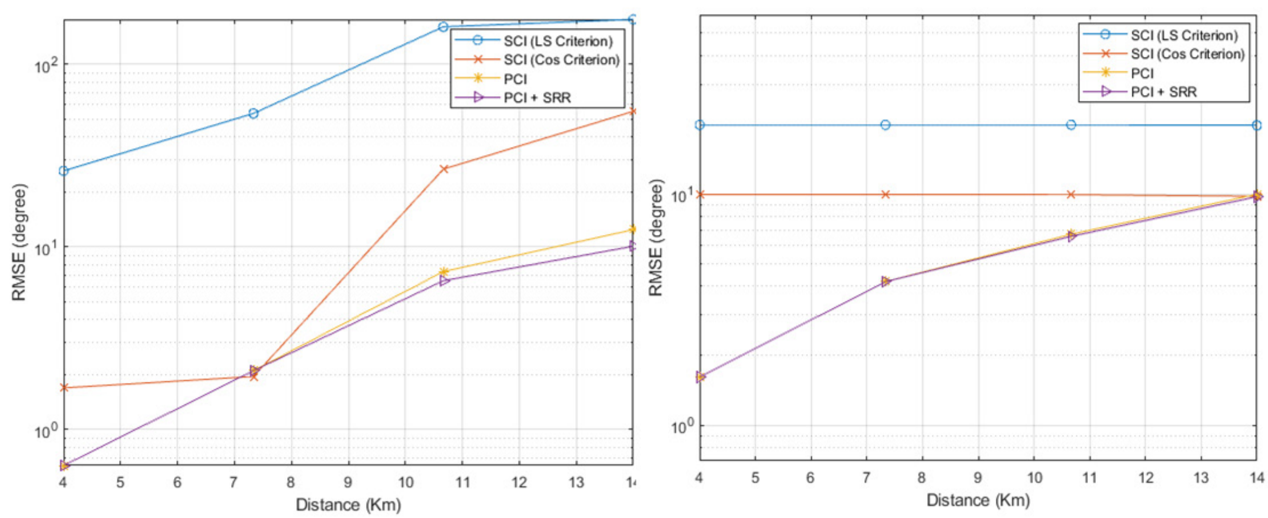

(a) (b)

Fig. 9 RMSE versus different distances of the source from the array in the multipath scenario. (a) Azimuth angle, (b) Elevation angle

frequency of these signals is 2.418 GHz and their bandwidth is 307.2 kHz. The transmitter power of the first signal is -30dB and the received power of the second signal is 3dB less than the received power of the first signal. The distance of this source is 1 km from the array.

- A broadband signal with a central frequency of 2.4025 GHz and a bandwidth of 3.0720 MHz, whose azimuth and elevation angles are 195° and 90°, respectively: The transmitter power is considered equal to -30dB. This source is located 700 m from the array.
- An FH signal with 9 random hops (so that they are available in the real-time bandwidth of the receiver) with a hopping rate equal to 750 hop/sec: Its azimuth angle is 45° and the elevation angle is equal to 75°, which is at a distance of 500 m from the array. The transmitter power is -30dB, and its bandwidth is 307.2 kHz.

All the mentioned signals have QPSK modulation, RRC pulse shape, and N_{re}=500. To implement the desired DOA algorithm (PCI or SCI), frequency spectrum analysis is performed in the instantaneous

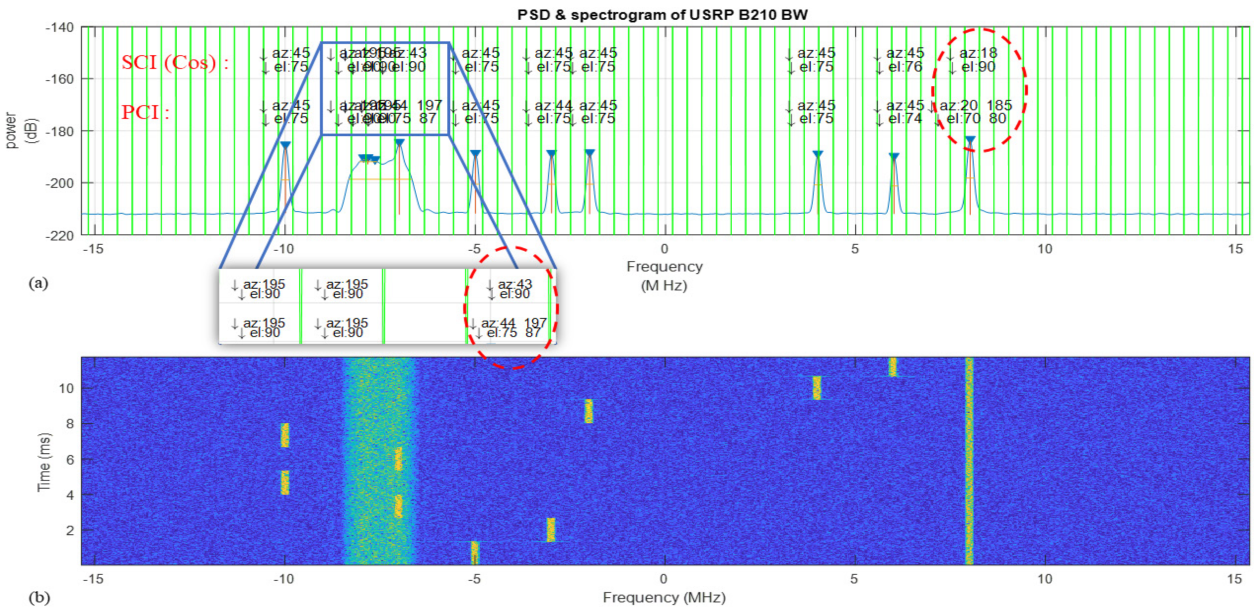

Fig. 10 DOA estimation results of some active subchannels of the real-time bandwidth of the USRP B210 receiver by PCI and SCI methods. (a) PSD spectrum along with DOA results, (b) Spectrogram or time-frequency waterfall spectrum.

bandwidth of the receiver to detect active subchannels according to Section III. Then, the desired DOA method is implemented in the active subchannels.

Fig. 10 shows the DOA results by implementing the PCI and SCI methods with the Cos criterion for some active subchannels detected on the real-time bandwidth of the receiver. As can be seen in the red dashed lines, the PCI method performs better than the SCI method in subchannels containing more than one active signal and presents a more accurate result.

Table 2. Final DOA estimation of WB/FH signals using the proposed clustering algorithm.

Number	Azimuth	Elevation	Cluster	Mean_Az	Mean_El
1	45	75	1	44.71	74.85
2	44	75	1	44.71	74.85
3	45	75	1	44.71	74.85
4	44	75	1	44.71	74.85
5	45	75	1	44.71	74.85
6	45	75	1	44.71	74.85
7	45	74	1	44.71	74.85
8	195	90	2	195	90
9	195	90	2	195	90
10	195	90	2	195	90
11	197	87	3	197	87

5.3 Proposed Modified K-means Performance in Final DOA Estimation of FH and WB Signals

In this section, a test example of the proposed clustering algorithm is presented in Table 2. The input to this experiment consists of the 2D DOAs, including the active subchannels corresponding to the FH and WB signals from the experiment related to Figure 10. As observed, the algorithm categorizes the data into three clusters, and then the mean of each cluster is calculated. Consequently, the third cluster, which consists of outlier data, is considered a single-member cluster and is excluded from the final DOA estimation of the WB signals.

Next, an experiment is conducted to compare the final DOA estimation methods for WB and FH signals in the real-time bandwidth of a USRP B210 receiver using the proposed improved K-means method, standard K-means, K-means++, and K-means proposed in [21] (K-means [21]). This experiment is performed assuming the same sources as in the previous section, with the difference that the three narrowband, WB, and FH sources have SNRs equal to 7, 10, and 5, respectively. The goal is to estimate the final 2D DOA of FH and WB signals from their corresponding detected active subchannels. The experiment has been done with L=500 independent Monte Carlo simulations, in which RMSE is defined in the following form:

$$\mathrm{RMSE}(\beta) = \sqrt{\frac{1}{LZ}\sum_{l=1}^{L}\sum_{z=1}^{Z}\left\|\hat{\beta}_{lz} - \beta_{lz}\right\|^2}\,, \quad (19)$$

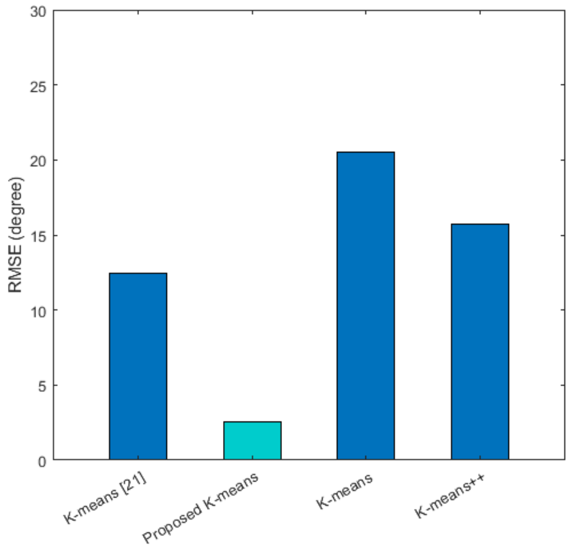

Fig. 11 RMSE versus clustering methods: K-means [21], proposed K-means, standard K-means, and K-means++.

where $\hat{\beta}$ is the 2D DOA estimation (azimuth and elevation angles) of the WB and FH signals, β is equal to the actual 2D DOA of the two WB and FH signals and Z is equal to the number of signals whose DOA must be estimated. Therefore, it is considered equal to 2.

The RMSE diagram according to different methods is drawn in Fig. 11. It can be seen that the proposed modified K-means method (Proposed K-means) has a better performance than other methods.

6 Conclusion

In this paper, a 2D DOA method based on CI was presented using lookup table expansion. Then, by considering the specifications of a USRP B210 receiver with two simultaneous channels and an SP9T switch, the reception of samples from each element of the proposed array was discussed. Additionally, an analysis for the PSD spectrum and spectrogram of the instantaneous bandwidth of the intended receiver was proposed to reduce calculations through the detection of active narrowband, WB, and FH signals in the subchannels of the optimal filter bank defined on the instantaneous bandwidth. Then, a modified K-means clustering method was proposed for the final estimation of the DOA of FH and WB signals. In the simulation section, the proposed 2D DOA estimation method was tested for receiving narrowband, WB, and FH signals by the proposed DF system. The simulation results show the improvement of DOA accuracy in multipath conditions through the proposed PCI method for DOA estimation of signals sent from far distances compared to the SCI method. It also shows the results of improving the accuracy of the final DOA estimation of FH and WB signals by the proposed modified K-means method compared to the standard K-means, K-means++ and K-means proposed in [21]. Future research could continue to design the antenna, investigate the multiple coupling effect between elements, investigate phase error due to hardware and calibration considerations, and combine the proposed DOA method with location finding techniques.

Conflict of Interest

The authors declare no conflict of interest.

Author Contributions

Both authors have actively participated in all stages of the research and have thoroughly reviewed and approved the final published version of the manuscript.

Funding

This research did not receive any specific grant from funding agencies in the public, commercial, or not-for-profit sectors.

Informed Consent Statement

Not applicable.

References

[1] A. Rembovsky, A. Ashikhmin, V. Kozmin, and S. Smolskiy, "Radio monitoring," *Problems, methods and equipment. Lecture notes in electrical engineering*. Springer, 2009.

[2] H. Zamani, H. Zayyani, and F. Marvasti, "An iterative dictionary learning-based algorithm for DOA estimation," *IEEE Communications Letters*, vol. 20, no. 9, pp. 1784-1787, 2016.

[3] S. Kulkarni, A. Thakur, S. Soni, A. Hiwale, M. H. Belsare, and A. B. Raj, "A comprehensive review of direction of arrival (DoA) estimation techniques and algorithms," *Journal of Electronics and Electrical Engineering*, pp. 138–186-138–186, 2025.

[4] M. Qu, W. Si, and R. Liu, "Array design and phase interferometer-based DOA estimation for diversely polarized antenna arrays," *Measurement, vol*. 242, p. 116222, 2025.

[5] P. Ramezanpour, M. Aghababaie, M. Mosavi, and D. de Andrés, "Multi-stage beamforming using DNNs," *Iranian Journal of Electrical & Electronic Engineering*, vol. 18, no. 2, 2022.

[6] T. Sallam, Q. Wang, and A. M. Attiya, "High-resolution multiple-source 2D DOA estimation using convolutional neural network with robustness to array imperfections," *IEEE Access*, 2024.

[7] S. Zheng et al., "Deep learning-based DOA estimation," *IEEE Transactions on Cognitive Communications and Networking*, 2024.

[8] V. S. Doan, T. Huynh-The, V. P. Hoang, and J. Vesely, "Phase-difference measurement-based angle

of arrival estimation using long-baseline interferometer," *IET Radar, Sonar & Navigation*, vol. 17, no. 3, pp. 449-465, 2023.

[9] S. S. Moghaddam, Z. Ebadi, and V. T. Vakili, "A novel DOA estimation approach for unknown coherent source groups with coherent signals," *Iranian Journal of Electrical and Electronic Engineering*, vol. 11, no. 1, pp. 8-16, 2015.

[10] A. M. Molaei and M. Hoseinzade, "High-performance 2D DOA estimation and 3D localization for mixed near/far-field sources using fourth-order spatiotemporal algorithm," *Digital Signal Processing*, vol. 100, p. 102696, 2020.

[11] C. Xu, Z. Wang, Y. Wang, Z. Wang, and L. Yu, "Three passive TDOA-AOA receivers-based flying-UAV positioning in extreme environments," *IEEE Sensors Journal*, vol. 20, no. 16, pp. 9589-9595, 2020.

[12] Y. Jiang and F. Liu, "Adaptive joint carrier and DOA estimations of FHSS signals based on knowledge-enhanced compressed measurements and deep learning," *Entropy*, vol. 26, no. 7, p. 544, 2024.

[13] M. Lin, Y. Tian, X. Zhang, and Y. Huang, "Parameter estimation of frequency-hopping signal in UCA based on deep learning and spatial time–frequency distribution," *IEEE Sensors Journal*, vol. 23, no. 7, pp. 7460-7474, 2023.

[14] I. Pokrajac, P. Okiljević, and N. Kozić, "An approach to design and development of a wideband direction finder simulator," *Scientific Technical Review*, vol. 66, no. 3, pp. 12-20, 2016.

[15] P. P. Vaidyanathan, "Multirate digital filters, filter banks, polyphase networks, and applications: a tutorial," *Proceedings of the IEEE*, vol. 78, no. 1, pp. 56-93, 1990.

[16] T. Ballal and C. J. Bleakley, "DOA estimation of multiple sparse sources using three widely-spaced sensors," in proc. *17th European Signal Processing Conference*, 2009: IEEE, pp. 1978-1982.

[17] M. Ahmed, R. Seraj, and S. M. S. Islam, "The k-means algorithm: A comprehensive survey and performance evaluation," *Electronics*, vol. 9, no. 8, p. 1295, 2020.

[18] A. E. Ezugwu et al., "A comprehensive survey of clustering algorithms: State-of-the-art machine learning applications, taxonomy, challenges, and future research prospects," *Engineering Applications of Artificial Intelligence*, vol. 110, p. 104743, 2022.

[19] A. Liu, Y. Zhou, Z. Li, Y. Xie, C. Zeng, and Z. Liu, "Simultaneous source number detection and DOA estimation using deep neural network and K2-means clustering with prior knowledge," *Electronics*, vol. 14, no. 4, p. 713, 2025.

[20] G. Shibin and S. Changyu, "The DOA of wideband signals estimation by using ESPRIT based on K-means," in proc. *2nd International symposium on instrumentation and measurement, sensor network and automation (IMSNA)*, 2013: IEEE, pp. 856-859.

[21] J. Ye et al., "A new frequency hopping signal detection of civil UAV based on improved k-means clustering algorithm," *IEEE Access*, vol. 9, pp. 53190-53204, 2021.

[22] F. A. Garcia et al., "Estimation of DOA for a Smart Antenna using a front-end based in FPGA foreseeing a SDR architecture," in proc. *First European Conference on Antennas and Propagation*, 2006: IEEE, pp. 1-4.

[23] S. Abeywickrama, L. Jayasinghe, H. Fu, S. Nissanka, and C. Yuen, "RF-based direction finding of UAVs using DNN," in proc. *IEEE International Conference on Communication Systems (ICCS)*, 2018: IEEE, pp. 157-161.

[24] A. A. Hussain, N. Tayem, A.-H. Soliman, and R. M. Radaydeh, "FPGA-based hardware implementation of computationally efficient multi-source DOA estimation algorithms," *IEEE Access*, vol. 7, pp. 88845-88858, 2019.

[25] S. Li, A. Liu, X. Xu, Y. Wang, Y. Yang, and L. Xia, "Radio interferometer with UAV and SDR payload for direction-finding of non-coherent emitter," *IEEE International Conference on Signal, Information and Data Processing (ICSIDP)*, 2024: IEEE, pp. 1-6.

[26] P. Tomikowski and G. Mazurek, "Acceleration of radio direction finder algorithm in FPGA computing platform," in proc. *23rd International Radar Symposium (IRS)*, 2022: IEEE, pp. 279-282.

[27] Z. Memarian and M. Majidi, "Multiple signals direction finding of IoT devices through improved correlative interferometer using directional elements," in proc. *Sixth International Conference on Smart Cities, Internet of Things and Applications (SCIoT)*, 2022: IEEE, pp. 1-6.

[28] R. Kudpik, K. Meksamoot, N. Siripon, and S. Kosulvit, "Design of a compact biconical antenna for UWB applications," in proc. *International Symposium on Intelligent Signal Processing and Communications Systems (ISPACS)*, 2011: IEEE, pp. 1-6.

[29] B. R. Jackson, S. Rajan, B. J. Liao, and S. Wang, "Direction of arrival estimation using directive antennas in uniform circular arrays," *IEEE Transactions on Antennas and propagation*, vol. 63, no. 2, pp. 736-747, 2014.

[30] *USRP B200/B210 Catalog*, Ettus Research, 2019.

[31] *P9T-500M40G-60-R-55-292FF-OPT1222 Catalog*, Quantic PMI.

[32] N. A. M. Razali, M. H. Habaebi, N. Zulkurnain, M. R. Islam, and A. Zyoud, "The distribution of path loss exponent in 3D indoor environment," *Int. J. Appl. Eng. Res*, vol. 12, no. 18, pp. 7154-7161, 2017.

[33] S. Lloyd, "Least squares quantization in PCM," *IEEE Transactions on Information Theory*, vol. 28, no. 2, pp. 129-137, 1982.

[34] G. A. Wilkin and X. Huang, "K-means clustering algorithms: implementation and comparison," in proc. *Second international multi-symposiums on computer and computational sciences (IMSCCS)*, 2007: IEEE, pp. 133-136.

Biographies

Z. Memarian was born in Qom, Iran, in 1993. She received the B.Sc. degree in Electrical Engineering in the Faculty of Electrical and Computer Engineering, Qom University of Technology, Qom, Iran, in 2016 and the M.Sc. degree in Electrical Engineering from the Kashan University, Kashan, Iran, in 2022.

M. Majidi received the B.Sc. degree in electrical engineering from Isfahan University of Technology, Isfahan, Iran, in 2004, and the M.S. and Ph.D. degrees in electrical engineering from Amirkabir University of Technology (Tehran Polytechnic), Tehran, Iran, in 2007 and 2014, respectively. In 2012, he joined the Communications and Networks Laboratory, Department of Electrical and Computer Engineering, National University of Singapore (NUS), Singapore, as a Visiting Ph.D. Student. In 2015, he worked as a researcher at the Iran Telecommunication Research Center (ITRC). Since 2016, he has been an assistant professor of the Department of Electrical and Computer Engineering, University of Kashan, Iran. Also, from January 2023 to September 2024, he worked as a senior communication system designer for Qualinx BV in Netherlands. His research interests include numerical and analytical optimization methods, intelligent reflecting surfaces, machine learning, wireless transceiver design, LPWAN, and GNSS.